Traffic flow reconstruction using mobile sensors and loop detector data

Juan C. Herrera*
Institute of Transportation Studies, Department of Civil and Environmental Engineering
University of California, Berkeley.

Alexandre M. Bayen†
Systems Engineering, Department of Civil and Environmental Engineering
University of California, Berkeley.

November 15, 2007

87th TRB Annual Meeting

Word count: 5715 words in text + 5 figures + 1 table = 7215 words

*Corresponding author: 116 McLaughlin Hall, Berkeley, CA 94720; jcherrera@berkeley.edu; Tel:510-642-7390.
†Assistant Professor. 711 Davis Hall, Berkeley, CA 94720; bayen@berkeley.edu; Tel:510-642-2468; Fax:510-643-5264.

Abstract

In order to develop efficient control strategies to improve traffic conditions on freeways, it is necessary to estimate the state of the traffic accurately in space and time. Using data collected from stationary detectors –such as loop detector stations– the density field can be currently reconstructed to a certain accuracy. Unfortunately, deploying this type of infrastructure is expensive, and its reliability varies based on public funding. This article proposes and investigates new algorithms that make use of data provided by mobile sensors, in addition to that collected by stationary detectors, to reconstruct traffic flow. Two approaches are proposed and evaluated with traffic data. The first approach is based on data assimilation methods (so-called nudging method or Newtonian relaxation) and the second is based on Kalman filtering. These approaches are evaluated using traffic data. Results show that the proposed algorithms appropriately incorporate the new data, improving significantly the accuracy of the estimates that consider loop detector data only.

1 INTRODUCTION

In order to develop efficient control strategies to improve traffic conditions on freeways, it is necessary to estimate the state of the traffic accurately in space and time. In particular, the knowledge of the density field or the velocity field is useful to determine bottleneck locations, physical extent of queues, and travel time. Using data collected from stationary detectors –such as loop detector stations– these fields can be currently reconstructed to a certain accuracy. Unfortunately, deploying this type of infrastructure is expensive, and its reliability varies.

New technology developments such as the *Global Positioning System* (GPS) allow cellular phones to broadcast their position and/or velocity in real time. If the cellular phone is located in a moving vehicle, the information collected from the phone can be used –in addition to (or instead of) the information provided by static sensors (e.g. loop detectors)– in traffic state estimation.

This new sensing technology has greatly impacted the transportation field, constituting a novel and rich source of traffic data. Maintenance problems common with stationary sensors (loop detectors mainly) do not appear with this technology. For public transportation agencies, there is no cost of deploying this new sensing technology, which is market driven. Personal devices (cellular phones) that people already have act as sensors, which has brought private companies into a field that has historically been monitored and managed by public agencies (encouraging partnerships between the public and private sector). Given the high penetration rate of cellular phones across the population –particularly in developing countries–, this new sensing technology has the potential of being deployed almost everywhere.

The problem of interest consists of finding new algorithms to make use of the data obtained from mobile sensors, in particular vehicles acting as probes –in addition to the data collected from stationary detectors– to estimate traffic state on freeways. The goal of this article is to incorporate mobile sensing information into traffic flow models so better estimates of traffic can be obtained.

The rest of the article is organized as follows. Background material is provided in Section 2, in which studies making use of data from loop detectors or probe vehicles are presented. Section 3 describes the proposed methods to address the problem of interest. These approaches were evaluated using traffic data, and the results are discussed in Section 4. Finally, some preliminary conclusions are presented in Section 5.

2 BACKGROUND

Depending on the way data is collected, two types of measurements can be used in traffic flow estimation. The first one consists in observing traffic flow at fixed locations (*Eulerian* measurements). This is the case of data collected from loop detectors stations. The second way is by following specific vehicle trajectories, which yields *Lagrangian* measurements (i.e. trajectory-based). Lagrangian data can be obtained using GPS technology inside cellular phones, or any tracking device providing position and velocity of specific vehicles.

Different methods are appropriate to reconstruct the density of vehicles on the freeway depending on the nature of collected data (Eulerian or Lagrangian). Traffic models and data collected from loop detectors (i.e. Eulerian data) can be used to reconstruct the density field in a fairly reasonable way. These models, however, have no explicit way of incorporating Lagrangian data into the modeling. The next sections summarize how Eulerian and Lagrangian sensors have been used in other studies to reconstruct traffic flow.

2.1 Eulerian sensing

Numerous freeways around the world, in particular in the US, have loop detector stations embedded in the pavement to collect traffic data. For each lane, these detectors aggregate information at a sample time (usually 20 or 30 seconds) for each lane. Vehicle counts, occupancy are among the information that a detector collects. This type of data has been used in different ways for several traffic applications and studies. In particular, some studies have used this type of data to perform traffic state estimation.

Gazis and Knapp in [1] and Szeto and Gazis in [2] are among the first studies that make use of Kalman filtering techniques to estimate the density on a section of freeway. The corresponding algorithms are based on the conservation of vehicle principle and they use vehicle counts and speeds at the boundaries of the section to perform the estimation.

Lin and Ahanotu in [3] validate the *Cell Transmission Model* (CTM) using data collected from loop detectors. The CTM is a traffic flow model proposed by Daganzo in [4] and [5]. It is a discretization of the *Partial Differential Equation* (PDE) proposed in the 1950's by Lighthill and Whitham [6] and Richards [7] (known as the LWR PDE) to describe the evolution of traffic flow over time and space. The CTM divides the highway in "cells" of length Δx and every Δt units of time the number of vehicles on each cell is updated according to the conservation of vehicles principle. The CTM transforms the nonlinear flux function into a nonlinear discrete operator. Muñoz et al. in [8] propose the *Switching-Mode Model* (SMM), which is a piecewise linearized version of the CTM. Using the framework of hybrid systems [9], the SMM combines discrete event dynamics (mode identification) with nonlinear continuous dynamics (density estimation). In [8] and [10], the authors test the proposed model using data collected from detectors on a stretch of highway I-210W in Pasadena, California.

Treiber and Helbing in [11] propose and test a method that "filters" data from detectors (density or velocities) to reconstruct traffic flow. In contrast with previous methods, this method does not take into account information about the traffic dynamics (such as the LWR PDE). It only considers the main propagation direction of the information to perform the estimation (downstream under free flow conditions and upstream when congestion arises).

2.2 Lagrangian sensing

Unlike Eulerian sensors, the use of Lagrangian sensors to reconstruct traffic flow has not been widely studied in transportation. Several studies have focused on technical and operational aspects of a probe system used to estimate travel times. Other studies have dealt with methodological aspects of travel time estimation and incident detection. Sanwal and Walrand in [12] propose an algorithm to estimate the average speed on a given link from probe speeds using a Bayesian approach (i.e. local speed estimation using Lagrangian speed measurement) in order to estimate travel time. The speeds estimated correlate well with the ones collected by loop detectors. Westerman et al. in [13] discuss the idea of fusing infrastructure-based loop detector data and non-infrastructure based probe vehicle data (i.e Eulerian and Lagrangian data) to obtain travel time estimations and to detect incident automatically. Ygnace et al. in [14] present analytical and simulation results to estimate travel time from individual speed measurements. Chu et al. in [15] use Kalman filtering techniques to combine point detection data and probe vehicle data into the travel time estimation. They propose an *Adaptive Kalman Filter* (AKF) based method that can dynamically estimate noise statistics of the system model by adapting to the real-time data. The evaluation shows improvements in travel time

estimation when compared with the case in which no probe data is available.

One of the first studies (to our best knowledge) which tried to incorporate Lagrangian data into the traffic state estimation problem was done by Nanthawichit et al. in [16], where the authors use Kalman filtering to improve estimations from traffic models that use only Eulerian data. Using Payne's traffic flow model and simulated data, they concluded that traffic state estimation improves when Lagrangian data is used. The authors also used this approach to predict travel times.

The reconstruction of velocity fields using Lagrangian data is common in other areas such as meteorology and oceanography. In these fields, the process of blending Lagrangian data and a dynamic model of the system is known as *data assimilation*. Terpstra et al. in [17] claim that data assimilation is not limited to physical processes, but it can also be used for prediction and modeling of behavior-based processes (car-drivers behavior in this case). Therefore, the extrapolation of these techniques to the transportation engineering problems appears to be very promising.

Data assimilation methods range from simple, suboptimal techniques such as direct insertion, statistical correction, and statistical interpolation to more sophisticated, optimal algorithms such as inverse modeling, variational techniques and a family of methods based on the Kalman filtering [18]. One of the simpler methods is the *nudging* (or Newtonian relaxation) method.

The nudging method relaxes the dynamic model of the system towards the observations. To this end, a source term proportional to the difference between the predicted and observed state is included in the constitutive equation $f(\boldsymbol{z}, x, t) = 0$ of the model (in the present case the LWR PDE):

$$f(\boldsymbol{z}, x, t) = \lambda(x, t) \cdot (\boldsymbol{z} - \boldsymbol{z^o}) \tag{1}$$

where x is the space variable, t is time, $\boldsymbol{z}$ is the state vector (in the present case car density), and $\boldsymbol{z^o}$ is the observation vector (measurements). The term $\lambda(x, t)$ is called nudging factor, which vanishes away from the measurement location and after the measurement time. Therefore, $\lambda(x, t)$ *nudges* the solution towards the observations closer to (x, t) when the observation is made.

Most of the data assimilation methods use boundary conditions. They must be known at some specific locations (usually at the boundaries of the computational domain). Thus, these methods make use of Eulerian data as well.

3 PROPOSED METHODS

The problem of interest for the present study is the traffic state estimation when Lagrangian data is available. This section describes the proposed approaches to address this problem.

Considering Eulerian data only, provided by loop detectors at the boundaries of the section under analysis, at time t the traffic flow model will provide a *first* estimate of the density field $\rho(x, t)$, denoted by $\hat{\rho}^-(x, t)$. At time t, Lagrangian sensors will provide the *observed* local density at some specific location x_i, denoted by $\rho^o(x_i, t)$ (the superscript o denotes *observation*). For these specific locations, the *first* estimate and the *observed* density will probably differ from each other. This difference $(\hat{\rho}^-(x_i, t) - \rho^o(x_i, t))$ will be used to compute a *second* estimate of the density everywhere at time t, denoted by $\hat{\rho}(x, t)$.

The present study proposes to use data assimilation techniques such as nudging or Kalman filtering techniques to obtain the *second* estimate $\hat{\rho}(x, t)$. The rest of this section is divided into three subsections. Section 3.1 explains how the observed local density can be obtained from Lagrangian measurements. A

more detailed description of both the nudging method and the Kalman filtering approaches is provided in the next subsections.

3.1 Computation of observed local density from Lagrangian data

Regular error-free measurements of vehicle position and velocity ($x_j(t)$ and $v_j(t)$, respectively, where j denotes a particular equipped vehicle) are assumed to be available from the sensing technology. Denoting the velocity fields by $v(x,t)$, individual measurements provide the knowledge of the observed velocity at location $x_j(t)$ at time t is the velocity of the vehicle at that location and time, i.e. $v^o\left(x_j(t),t\right) = v_j(t)$, where the superscript o denotes *observation*. This assumption may not be appropriate when dealing with multi-lane freeways, where different lanes might have different speeds. As a first approach, however, we treat the freeway as a single traffic stream.

Using the fundamental diagram, $v^o\left(x_j(t),t\right)$ can be used to obtain the density at the point of measurement, $\rho^o\left(x_j(t),t\right)$. In reality, $\rho^o\left(x_j(t),t\right)$ is not the observed density but an estimate based on the fundamental diagram.

If a triangular fundamental diagram is used, there is a problem when $v_j(t) = v_f$, where v_f is the free flow speed. Same combinations of flow and density under free flow conditions have the same free flow speed. That is, under free flow conditions it is not possible to observe the local density through speed measurements. For these cases, we will not consider the observation. Since the traffic flow model behaves well under free flow conditions, this should not be a significant issue. Therefore, if $v_j(t) = v_f$ free flow conditions are assumed and the density predicted by the model is assumed to be equal to the observed density (and then the observation is dismissed).

3.2 Data assimilation: nudging method or Newtonian relaxation

For its simplicity and computational efficiency, the nudging method –briefly outlined in Section 2.2– is appealing.

The dynamic traffic flow model is given by the LWR PDE. The boundary conditions will be provided by loop detector stations (Eulerian data), while some equipped vehicles –i.e. the vehicles equipped with tracking technology– will provide their position and velocity over time (Lagrangian data).

Traffic flow model. The traffic flow model is the LWR PDE:

$$\frac{\partial \rho}{\partial t} + \frac{\partial q(\rho)}{\partial x} = 0 \tag{2}$$

with the boundary conditions

$$\rho(a,t) = \rho_a(t) \text{ and } \rho(b,t) = \rho_b(t), \text{ with } t \in (0,T) \tag{3}$$

and the initial condition

$$\rho(x,0) = \rho_0(x), \text{ with } x \in (a,b) \tag{4}$$

$\rho(x,t)$ represents the vehicle density in vehicles per distance and $q(\rho)$ is the fundamental diagram (flux function), which in this study will be assumed to be concave (triangular for the implementation). For a

proper characterization of Equation (2), weak boundary conditions are required, and boundary conditions in (3) cannot be used as such. Boundary conditions only apply on the boundary of the section where characteristics are entering the computational domain. Weak boundary conditions for the specific case of the LWR PDE can be found in [19]:

$$\begin{cases} \rho(a,t) = \rho_a(t) \text{ or} \\ q'\left(\rho\left(a,t\right)\right) \leqslant 0 \text{ and } q'\left(\rho_a\left(t\right)\right) \leqslant 0 \text{ or} \\ q'\left(\rho(a,t)\right) \leqslant 0 \text{ and } q'\left(\rho_a(t)\right) \geqslant 0 \text{ and } q\left(\rho(a,t)\right) \leqslant q\left(\rho_a(t)\right) \end{cases}$$

and

$$\begin{cases} \rho(b,t) = \rho_b(t) \text{ or} \\ q'\left(\rho\left(b,t\right)\right) \geqslant 0 \text{ and } q'\left(\rho_b\left(t\right)\right) \geqslant 0 \text{ or} \\ q'\left(\rho(b,t)\right) \geqslant 0 \text{ and } q'\left(\rho_b(t)\right) \leqslant 0 \text{ and } q\left(\rho(b,t)\right) \leqslant q\left(\rho_b(t)\right) \end{cases}$$

In practice, these boundary conditions are implemented using *ghost cells*.

Nudging method in traffic flow. From Equation (1), the nudging method consists in adding a source term to the dynamic model in Equation (2):

$$\frac{\partial \rho}{\partial t} + \frac{\partial q(\rho)}{\partial x} = -\sum_{j=1}^{J} \lambda\left(x - x_j(t), t\right) \cdot \left(\rho\left(x_j(t), t\right) - \rho^o\left(x_j(t), t\right)\right) \tag{5}$$

The summation over the index j in the RHS of Equation (5) accounts for the J different vehicles equipped with Lagrangian sensors. A possible expression for the nudging factor $\lambda\left(x,t\right)$ can be found in [20] and is given by:

$$\lambda(x,t) = \begin{cases} \frac{1}{T_a} \exp\left(-\frac{x^2}{X_{\text{nudge}}^2}\right) \exp\left(-\frac{t-t^o}{T_d}\right) & \text{if } x \leqslant \alpha X_{\text{nudge}} \text{ and } t \geqslant t^o \\ 0 & \text{otherwise} \end{cases} \tag{6}$$

In Equation (6), T_a is the timescale and determines the strength of the nudging factor, and t^o is the observation time. T_d and X_{nudge} reflect how the effect of any observation decreases over time and space, respectively (they determine how fast the two exponential terms go to zero). The coefficient α is a positive number that depends on the application, and reflects the zone of influence of the measurements. In our context, the nudging term "adds" or "removes" vehicles from the freeway depending on whether the model underestimates or overestimates the number of vehicles on the freeway.

Implementation issues. For implementation purposes, the LWR PDE needs to be discretized. To this end, the freeway section is divided into I cells (each one of length Δx distance units, and denoted by i), and time is divided into H time steps (each one of length Δt time units, and denoted by h). In order to meet the *Courant-Friedrichs-Lewy* (CFL) stability condition [21] –which states that no vehicle can travel more than one cell in one time step– the condition $\Delta t \cdot v_f \leqslant \Delta x$ should be met. At every time step the model estimates the density in each cell according to the following expression:

$$k_i^{h+1} = k_i^h - r\left(q_{i+1}^h - q_i^h\right) \qquad i = 1, 2, \ldots, I \text{ and } h = 0, 1, \ldots, H-1. \tag{7}$$

k_i^h is density in cell i at time h, q_i^h is the flow into cell i between time h and $h+1$, and r is the inverse of the speed needed to travel one cell in exactly one time step (i.e. $r = \frac{\Delta t}{\Delta x}$). q_i^h depends nonlinearly on k_i^h and k_{i-1}^h. The Godunov scheme [22] will be used to solve (7), and $q_i^h = q_G\left(k_{i-1}^h, k_i^h\right)$ where q_G is the Godunov flux defined as follows:

$$q_G(k_1,k_2) = \begin{cases} q(k_2) & \text{if } k_c < k_2 < k_1, \\ q(k_c) & \text{if } k_2 < k_c < k_1, \\ q(k_1) & \text{if } k_2 < k_1 < k_c, \\ \min(q(k_1), q(k_2)) & \text{if } k_1 \leqslant k_2. \end{cases}$$

k_c is the *critical density*, and it corresponds to the point at which the flux reaches its only maximum (the flux function is concave). The discretization of the nudging term needs to be added to Equation (7). The final expression for the model is as follows:

$$\begin{aligned} k_i^{h+1} &= k_i^h - r\left(q_G\left(k_i^h, k_{i+1}^h\right) - q_G\left(k_{i-1}^h, k_i^h\right)\right) - \Delta t \sum_{j=1}^{J} \sum_{t_p^j \in \mathcal{S}_j^h} \lambda\left(x_i - x_j\left(t_p^j\right), h\Delta t\right) \cdot \\ & \left[\hat{\rho}^-\left(x_j\left(t_p^j\right), t_p^j\right) - \rho^o\left(x_j\left(t_p^j\right), t_p^j\right)\right] \quad i = 1,2,\ldots,I \text{ and } h = 0,1,\ldots,H-1. \end{aligned} \tag{8}$$

The notation introduced in Equation (8) is explained below:

- J: total number of equipped vehicles,
- x_i: location of the beginning of cell i, $x_i = x_0 + (i-1)\cdot\Delta x$, for $i = 1,2,\ldots,I$, where x_0 is the beginning of the section of interest,
- t_p^j: time when the p-th observation from vehicle j occurs (in time units),
- $\mathcal{S}_j^h$: set of all the observations times of vehicle j that are less than or equal to the time elapsed until the h-th time step, i.e. $\mathcal{S}_j^h = \{t_p^j : 0 < t_p^j \leqslant h\cdot\Delta t\}$, and
- $\hat{\rho}^-\left(x_j\left(t_p^j\right), t_p^j\right) = \left(1-\theta_p^j\right)\cdot k_{i_{pj}}^{h_p^j} + \theta_p^j \cdot k_{(i_{pj}+1)}^{h_p^j}$, where:
  - h_p^j : time step when the p-th observation from vehicle j occurs (in time step units), i.e. $h_p^j = \lceil \frac{t_p^j}{\Delta t} \rceil$ (because of roundoff error of h_p^j, the algorithm might exhibit some lag of duration less than Δt in sensing),
  - i_{pj} : cell where vehicle j is located at time t_p^j, $i_{pj} = \lceil \frac{x_j(t_p^j) - x_0}{\Delta x} \rceil$, where $x_j(t_p^j) > x_0$, and
  - $\theta_p^j = \frac{x_j(t_p^j) - x_{i_{pj}}}{\Delta x}$, where $x_{i_{pj}} \leqslant x_j(t_p^j) \leqslant x_{(i_{pj}+1)}$.

The last term in the RHS of Equation (8) is the discrete version of the nudging factor times the difference between estimated and measured density (terms inside the square brackets). The density estimate at location $x_j(t_p^j)$ is based on linear interpolation between the density at the closest points –on the grid– to $x_j(t_p^j)$. The nudging factor is given by Equation (6), after substituting $x - x_j(t)$ by $x_i - x_j\left(t_p^j\right)$ and t by $h\Delta t$.

As pointed out earlier on, weak boundary conditions are required for a proper characterization of the solution of the LWR PDE in (2). For implementation purposes, one ghost cell is inserted at each boundary of the section. The ghost cells contain the boundary conditions, and they allow the first and last cells of the computational domain to be updated depending on the existing traffic conditions (free flow, congested, or a mix of the two). This approach was successfully implemented and tested by Strub and Bayen in [19] with traffic data collected from loop detectors. The equations for the ghost cells ($i = 0$ and $i = I + 1$) and for the initial conditions ($h = 0$) are given by Equation (9) and (10), respectively:

$$k_0^h = \frac{1}{\Delta t}\int_{(h-1)\Delta t}^{h\Delta t} \rho_a(t)dt \quad \text{and} \quad k_{I+1}^h = \frac{1}{\Delta t}\int_{(h-1)\Delta t}^{h\Delta t} \rho_b(t)dt \quad h = 0, 1, \ldots, H-1 \tag{9}$$

$$k_i^0 = \frac{1}{\Delta x}\int_{x_{i-1}}^{x_i} \rho_0(x)dx \quad i = 1, 2, \ldots, I. \tag{10}$$

3.3 Kalman filtering

Kalman filtering is a recursive method to estimate the state of a discrete process governed by a linear stochastic dynamical system. The estimate is such that its covariance is minimized. This section describes how Kalman filtering techniques can be used for the purposes of this work.

State space representation. The state space representation of the system consists in two equations: the dynamic (or state) equation and the measurement (or observation) equation. The dynamic equation describes how the state of the process (density in this case) evolves and is given by Equation (7), with $q_i^h = q_G\left(k_{i-1}^h, k_i^h\right)$. Since q_G is nonlinear, the SMM is used. Depending on the mode detected, the dynamic equation is chosen. This constitutes one of the main differences with respect to the nudging method described before, where no mode identification is performed (the method does not assume anything about freeway conditions).

If only the situations in which the whole section is either under free flow or congested are considered, the dynamic equation reads as follows (using the same notation as before):

$$k_i^{h+1} = \begin{cases} k_{i-1}^h & \text{if free flow} \\ (1-\delta)k_i^h + \delta k_{i+1}^h & \text{if congested} \end{cases} \quad i = 1, 2, \ldots, I \text{ and } h = 0, 1, \ldots, H-1. \tag{11}$$

where $\delta = w/v_f$, and w is the backward shockwave speed. Equation (11) assumes that every cell has the same length $\Delta x = v_f \Delta t$ and the same fundamental diagram, and that there is no creation or loss of vehicles at middle points (i.e. no ramps). For a more general formulation for these two cases (and three other cases that consider a combination of free flow and congested modes), the reader is referred to [23]. In matrix form, Equation (11) can be written as:

$$\boldsymbol{k}_{h+1} = A_h \cdot \boldsymbol{k}_h + B_h \cdot u_h + \boldsymbol{w}_h \tag{12}$$

Bold letters represent vectors. The vector $\boldsymbol{k}_h = [k_1^h \;\; k_2^h \;\; \ldots \;\; k_I^h]^T$ is the state vector at time step h, and matrices A_h and B_h are time-varying in the sense that they depend on the mode m at time step h (for

instance, $m = 1$ in free flow mode, $m = 2$ in congested mode). The term $\boldsymbol{w}_h$ represents the error of the state equation (caused by false or missed counts –because of lane changing manoeuvres for instance– at boundaries). The input u_h is a scalar and it is related to the measurements obtained at the boundaries of the computational domain (used to compute the density on the first or last cell under free flow or congested mode, respectively). In fact, if the whole section is either under free flow or congested mode:

$$u_h = \begin{cases} k_0^h, & \text{if free flow } (m = 1) \text{ on the section during } h; \\ k_{I+1}^h, & \text{if congested } (m = 2) \text{ on the section during } h. \end{cases} \tag{13}$$

where k_0^h and k_{I+1}^h come from Equation (9). Initial conditions k_i^0 are the same as in Equation (10).

The measurement or observation equation compares the observed values of the state variables with the ones predicted by the model. This equation is as follows:

$$\boldsymbol{y}_h = C_h \cdot \boldsymbol{k}_h + \boldsymbol{v}_h \tag{14}$$

$\boldsymbol{y}_h$ is the observed vector, and $\boldsymbol{v}_h$ is the measurement error (which constitutes another difference with respect to the nudging method, in which the observed density is assumed to be perfect or error free). Kalman filtering also assumes that $\boldsymbol{w}_h$ and $\boldsymbol{v}_h$ are independent and normally distributed with zero mean. The matrix C_h is time dependent. The size and elements of C_h depend on where the Lagrangian observations at h are coming from, and it contains only zeros and ones (it is assumed that the local density can be observed from Lagrangian sensors). Lagrangian observations are coming from different cells, and also the number of observations between consecutive time steps might be different. Thus, the observed vector $\boldsymbol{y}_h$ in Equation (14) will have different dimensions at different time steps. The latter implies that matrix C_h will also have different dimensions at every time step.

In summary, the dynamic or state equation and the measurement or observation equation of the system are given by Equation (12) and (14), respectively.

Solution method: Kalman filtering. Let us use the following notation:

- $\hat{\boldsymbol{k}}_h^-$: *a-priori* state estimate of $\boldsymbol{k}_h$,
- $\hat{\boldsymbol{k}}_h$: *a-posteriori* state estimate of $\boldsymbol{k}_h$,
- P_h^-: *a-priori* estimate error covariance, where $\boldsymbol{e}_h^- = \boldsymbol{k}_h - \hat{\boldsymbol{k}}_h^-$ is the *a-priori* estimate error,
- P_h: *a-posteriori* estimate error covariance, where $\boldsymbol{e}_h = \boldsymbol{k}_h - \hat{\boldsymbol{k}}_h$ is the *a-posteriori* estimate error.

Kalman filtering provides a set of recursive equations to estimate the vector state. The equations are as follows:

$$\hat{\boldsymbol{k}}_{h+1}^- = A_h \cdot \hat{\boldsymbol{k}}_h + B_h \cdot u_h \tag{15}$$

$$P_{h+1}^- = A_h \cdot P_h \cdot A_h^T + Q \tag{16}$$

$$F_{h+1} = P_{h+1}^- \cdot C_{h+1}^T \left[C_{h+1} \cdot P_{h+1}^- \cdot C_{h+1}^T + R \right]^{-1} \tag{17}$$

$$\hat{\boldsymbol{k}}_{h+1} = \hat{\boldsymbol{k}}_{h+1}^- + F_{h+1} \left(\boldsymbol{y}_{h+1} - C_{h+1} \cdot \hat{\boldsymbol{k}}_{h+1}^- \right) \tag{18}$$

$$P_{h+1} = \left(I - F_{h+1} \cdot C_{h+1} \right) P_{h+1}^- \tag{19}$$

Initial conditions $\hat{\boldsymbol{k}}_0$ and P_0 are assumed to be known. Q and R are the covariance matrix of the process and measurement error, respectively. F_h is known as the *Kalman filter gain* at time step h. The matrix C_h have different dimensions at every time step, which implies variable dimension of covariance matrix R.

Implementation issues. As before, the section is divided in I cells of length Δx and the simulation period is divided in H time steps of length Δt each, such that Δx and Δt satisfy the CFL stability condition. The state vector contains the density in each cell. At the beginning of each time step the traffic conditions on the network need to be identified (in order to determine the set of matrices A and B to use).

Once the mode has been identified at the beginning of time step $h + 1$, Equation (15) and (16) are used to obtain the *a-priori* density estimate and covariance, respectively (using the Eulerian data provided from detector stations). At this point, Lagrangian data becomes available to the model, i.e. the observed density at time $h + 1$ will be known for some cells (the quantity and position of the Lagrangian sensors at $h + 1$ will determine how many and for which cells the density is observed). With this information, the observed vector $\boldsymbol{y}_{h+1}$ and matrix C_{h+1} can be constructed. Then, the Kalman filter gain is computed using Equation (17). Finally, the *a-posteriori* density estimate and its covariance are obtained using Equation (18) and (19), respectively. In case no observation is available at time $h+1$, the matrix C_{h+1} is set equal to zero, which implies that the Kalman gain is also zero, and therefore the *a-posteriori* density estimate is equal to the *a-priori* density estimate.

4 RESULTS

The two approaches described in Section 3 are implemented with traffic data to evaluate their respective performance. The performance is evaluated in terms of the ability of the models to estimate three variables derived from the density field: number of vehicles between two points in space, density profile at middle location, and travel time to travel through the entire section.

Traffic data from the *Next Generation Simulation* (NGSIM) project [24] is used to evaluate the proposed approaches. The data consist of the trajectory for every vehicle that enter a stretch of US Highway 101S in Los Angeles, CA, during 45 minutes (from 7:50am to 8:35am) . Figure 1 illustrates the location of interest. The site is approximately 0.4 miles in length, with 5 mainline lanes. An auxiliary lane exists between the on-ramp and the off-ramp. Transition from free flow to congested mode happens during the first 12-15 minutes (i.e. part of the section was in the free flow mode while the rest was in the congested mode).

For implementation purposes, only the two left-most lanes were considered. The whole section (2040 ft) has been divided into $I = 17$ cells of $\Delta x = 120$ ft each, and the total simulation time (2634 sec) has been divided into $H = 2195$ time steps of $\Delta t = 1.2$ seconds each. Parameters of the fundamental diagram were extracted from PeMS[1].

For simplicity, no mode identification was performed in the Kalman filtering implementation. The whole section was assumed to be congested all the time. Four different scenarios were tried depending on how Lagrangian data is created. Some proportion p of the trajectories are chosen (randomly) as equipped vehicles. These vehicles are reporting their position and speed every time interval T, and the reported speed

[1]Assuming a triangular shape: $q_{\max} = 2040$ vphpl, $k_j = 205$ vpmpl, $k_c = 30$ vpmpl, $v_f = 68$ mph, and $w = -11.6$ mph.

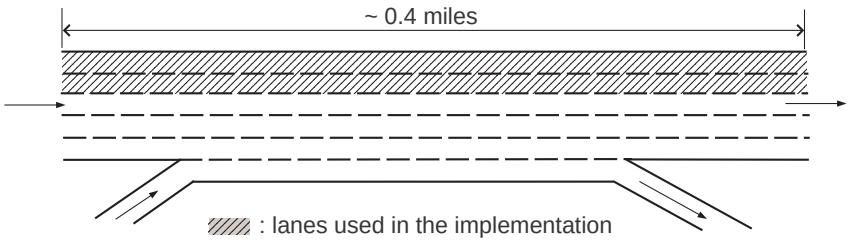

Figure 1: NGSIM site.

is the average speed over the last τ seconds. The values chosen for p, T, and τ determine the total number of Lagrangian measurements created for each of the four cases investigated (see Table 1).

Travel time for the section of interest is about 2 minutes under congested conditions. Thus, cases 1 and 3 assume that each equipped vehicle sends only one report while it is traveling the section. Continuous tracking for equipped vehicles is assumed in cases 2 and 4. Because of privacy issues, these two cases might not be a feasible solution in the future. They were investigated, however, to evaluate the potential of the methods proposed.

For comparison purposes, a model that uses *Eulerian data only* (EDO) was also implemented according to the numerical scheme proposed by Strub and Bayen in [19]. Figures 2, and 3 compare the true or observed evolution of the number of vehicles on the section with the estimates from the approaches.

Figure 2 compares the results using EDO with those from the proposed approaches under case 4 (i.e assuming that 20% of the vehicles are equipped and their speed is sampled continuously). The inclusion of Lagrangian data in the estimation process improves the accuracy of the estimates, regardless of the method used (Kalman filtering at the top and nudging method at the bottom). Both approaches appropriately incorporate the Lagrangian data into the model.

When both approaches use the same Lagrangian data, Kalman filtering yields more accurate estimates. The same results are found when the approaches are compared under any of the other three cases. Since the observed density has some error –as stated in Section 3.1, the observed density is actually an estimate, based on the fundamental diagram–, Kalman filtering's capability of handling an error in the observed density – see Equation (14)– might explain its slightly better performance (the nudging method assumes that the observed density is perfect, i.e. it has no error). However, the advantage of making no assumption about the freeway state (i.e. no mode identification needs to be performed) makes the results from the nudging method encouraging.

Figure 3 compares the Kalman filtering approach for the four different cases (i.e. assuming different penetration rates and sampling rates). The top graph contains the estimation for cases 2 and 4. The graph at the bottom contains the same curves but for cases 1 and 3. For low penetration rates (cases 1 and 2), the estimates are accurate as long as the sampling rate is high. For low sampling rates (cases 1 and 3), the estimates are not as accurate even when the penetration rate is high. As expected, the best results are achieved under case 4, when the amount of Lagrangian data is the highest.

The fifth column in Table 1 shows the *Root Mean Square Error*[2] (RMSE) of the estimation of the number

[2]The RMSE is defined as: RMSE $= \sqrt{\frac{\sum_h (\hat{z}_h - z_h)^2}{H}}$ where $\hat{z}_h$ and z_h are the estimator and its actual value at time step h, respectively.

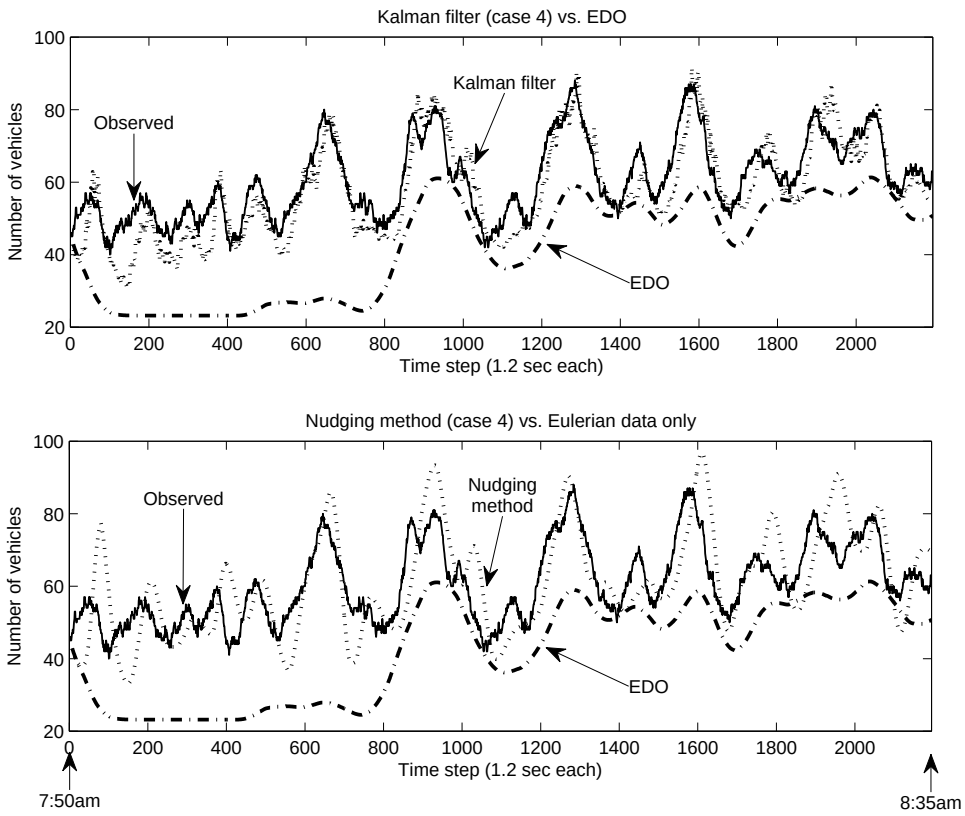

Figure 2: Estimation improvement when Lagrangian data is available.

of vehicles for both approaches and the four cases used. The table is sorted according to the seventh column.

In terms of the density profile and travel time estimation, the qualitative results are the same as before. Figure 4 shows the true or observed density profile at a middle point (extracted from vehicle trajectories and then smoothed) and the estimated profile for three different cases. The sixth column in Table 1 presents the RMSE's in terms of the density profile at a specific point in the middle of the section. Again, high penetration rates and high sampling rates achieve the best performance, and the use of Lagrangian data only improves estimations.

Figure 5 compares the real travel times (each dot corresponds to one vehicle) with the ones computed using the density field estimation. Travel time at time step h is the sum of each cell travel time at time step h. To compute each cell travel time at h, the density of each cell at h is converted into velocity (using the fundamental diagram). Knowing the velocity and the length of each cell, the travel time is computed.

Because of the time frame used and the short length of the section, the true or observed curves for the number of vehicles, density profile, and travel time show a large amplitude oscillatory behavior. Nevertheless, the proposed approaches show good fidelity to the trend in this *extreme* case. It is expected that with

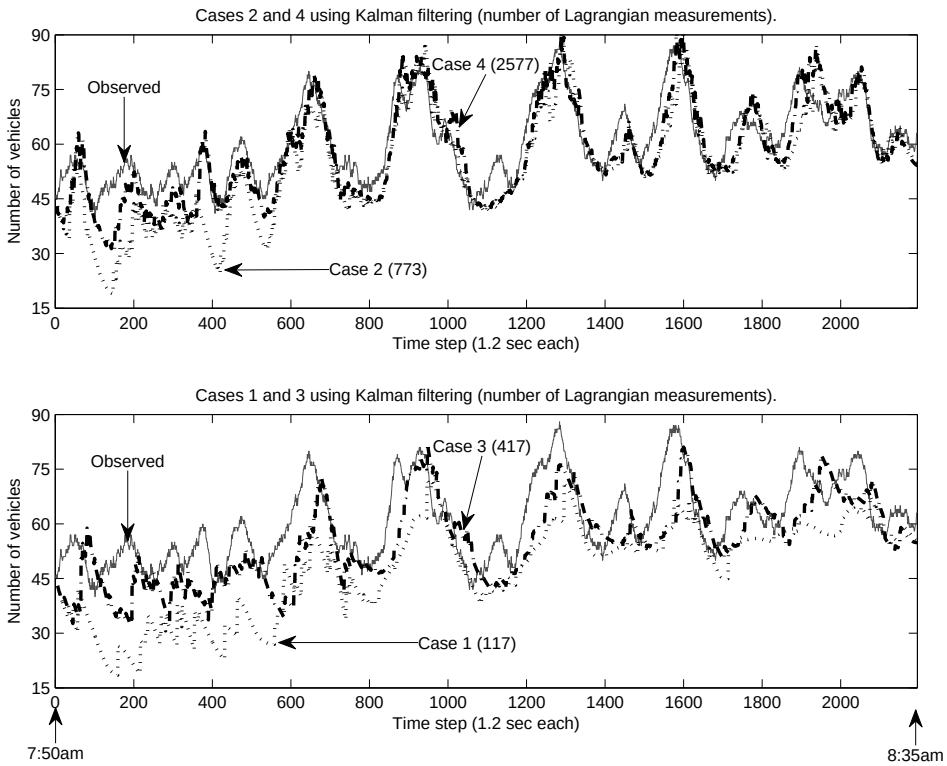

Figure 3: Comparison of high vs. low penetration and sample rates.

Table 1: RMSE using both approaches and different penetration rates and sampling rates.

						RMSE	
Method	Case	p (%)	T (sec)	τ (sec)	# of Lagrangian measurements	Number of vehicles	Density profile
KF	4	20	10	10	2577	6.6	12.7
KF	2	5	10	10	773	9.8	24.4
NM	4	20	10	10	2577	9.8	19.3
KF	3	20	600	30	417	10.4	23.9
NM	2	5	10	10	773	11.6	31.5
NM	3	20	600	30	417	12.1	32.3
KF	1	5	600	30	117	15.7	43.5
NM	1	5	600	30	117	17.7	46.9
EDO	N/A	N/A	N/A	N/A	N/A	21.3	57.8

less variability the results from both approaches should be at least as accurate as in this case. The results when EDO is used should improve as well. Therefore, the gap between EDO and the proposed approaches

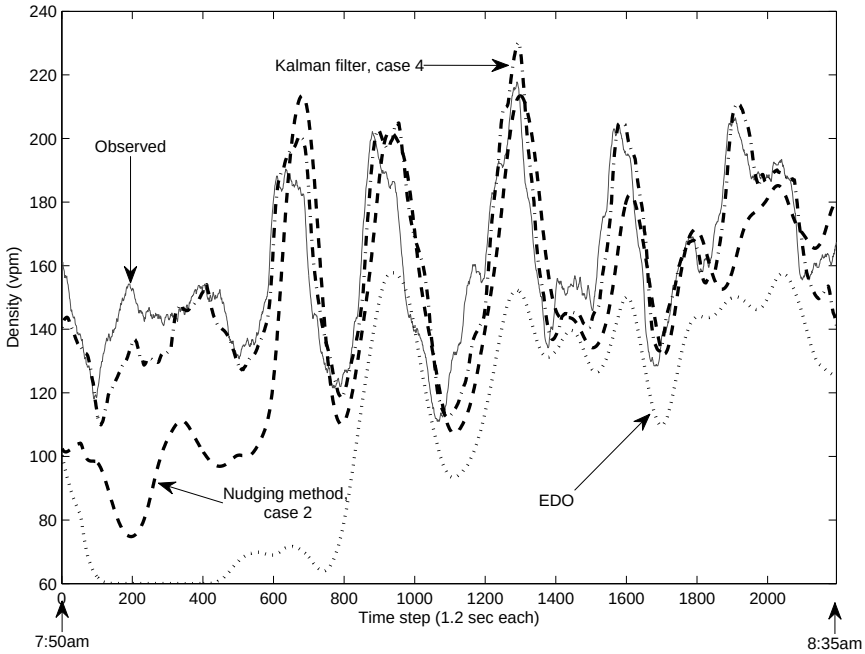

Figure 4: Density profile at middle location (cell 9).

should be smaller.

5 Final comments

Considering the limitations and special features of the NGSIM data set, results shown in Section 4 are promising. From the graphs and tables shown in Section 4, the following preliminary conclusions can be drawn:

- The use of Lagrangian data improves current estimations of the density field. As a result, more accurate estimates for the number of vehicles on the section and for travel times can be obtained.
- Even though both approaches appropriately incorporate Lagrangian data in the model, the Kalman filtering approach performs slightly better than the nudging method. However, the fact that no mode identification is performed –and the good results obtained– makes the nudging method an attractive method to be implemented in transportation.
- The more Lagrangian observations are available, the better accuracy can be achieved in the estimates. Best results are obtained for case 4, while worst results are achieved for case 1 (regardless of the approach used). Both approaches yield better results for case 2 than for case 3, implying that the number of Lagrangian measurements determines the accuracy of the estimates.

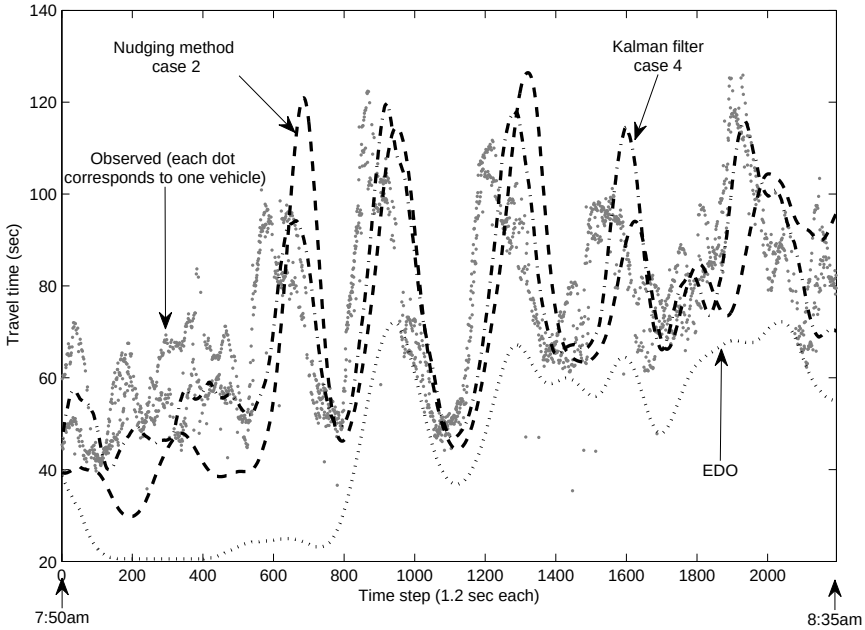

Figure 5: Travel time predictions.

- Some specific traffic features –like traffic oscillations or instabilities– are hard to capture with static detectors, specially when the spacing between the detectors is big. Information collected from individual vehicles over time and space can be helpful in this sense.

These conclusions are preliminary and more analysis needs to be done in order to draw some final conclusions. To this end, an extension to this research is being performed, where vehicle trajectories will be extracted from a microsimulation and then used to evaluate the proposed approaches (in the same manner as in Section 4). The use of cellular phones broadcasting their position and velocity will constitute the last level of evaluation of the proposed approaches.

Improvement in the computation of the observed density from Lagrangian data, and inclusion of error or noise in the nudging method (for the observed density) are among future challenges this research poses.

Acknowledgements

The authors would like to thank NGSIM for providing the vehicle trajectories used in this study and Saneesh Apte from CCIT for processing the data and computing sensor occupancies and speeds from the NGSIM vehicle trajectories. Also thanks to Issam Strub, Eric Lew and Shuo Yang for their involvement on different stages of this study. Finally, JD Margulici is acknowledged for providing CCIT support and fruitful discussion.

References

[1] D. Gazis and C. Knapp. On-line estimation of traffic densities from time-series of flow and speed data. *Transportation Science*, 5(3):282–301, 1971.

[2] M. Szeto and D. Gazis. Application of Kalman filtering to the surveillance and control or traffic systems. *Transportation Science*, 6(4):419–439, 1972.

[3] W-H. Lin and D. Ahanotu. Validating the basic cell transmission model on a single freeway link. PATH Technical Note 95-3, Institute of Transportation Studies, University of California, Berkeley, 1994.

[4] C. Daganzo. The cell transmission model: a dynamic representation of highway traffic consistent with the hydrodynamic theory. *Transportation Research B*, 28(4):269–287, 1994.

[5] C. Daganzo. The cell transmission model, Part II: Network traffic. *Transportation Research B*, 29(2):79–93, 1995.

[6] M.J. Lighthill and G.B. Whitham. On kinematic waves II. A theory of traffic flow on long crowded roads. In *Proceedings of the Royal Society*, volume A 229, pages 317–345, 1955.

[7] P.I. Richards. Shock waves on the higway. *Operation Research*, 4:42–51, 1956.

[8] L. Muñoz, X. Sun, R. Horowitz, and L. Alvarez. Traffic density estimation with the cell transmission model. In *Proceedings of the 2003 American Control Conference*, pages 3750–3755, Denver, CO, June 2003.

[9] C. Tomlin, J. Lygeros, and S. Sastry. A game theoretic approach to controller design for hybrid systems. In *Proceedings of the IEEE*, volume 88, July 2000.

[10] X. Sun, L. Muñoz, and R. Horowitz. Highway traffic state estimation using improved mixture Kalman filters for effective ramp metering control. In *Proceedings of the* 42nd *IEEE Conference on Decision and Control*, pages 6333–6338, Maui, HI, December 2003.

[11] M. Treiber and D. Helbing. Reconstructing the spatio-temporal traffic dynamics from stationary detector data. *Cooper@tive Tr@nsport@tion Dyn@mics*, 1:3.1–3.24, 2002.

[12] K.K. Sanwal and J. Walrand. Vehicles as probes. California PATH Working Paper UCB-ITS-PWP-95-11, Institute of Transportation Studies, University of California, Berkeley, 1995.

[13] M. Westerman, R. Litjens, and J-P. Linnartz. Integration of probe vehicle and induction loop data –estimation of travel times and automatic incident detection. PATH Research Report UCB-ITS-PRR-96-13, Institute of Transportation Studies, University of California, Berkeley, June 1996.

[14] J-L. Ygnace, C. Drane, Y.B. Yim, and R. de Lacvivier. Travel time estimation on the San Francisco Bay Area network using cellular phones as probes. California PATH Working Paper UCB-ITS-PWP-2000-18, Institute of Transportation Studies, University of California, Berkeley, 2000.

[15] L. Chu, S. Oh, and W. Recker. Adaptive Kalman filter based freeway travel time estimation. In 84th *TRB Annual Meeting*, Washington D.C., January 9-13 2005. Transportation Research Board.

[16] C. Nanthawichit, T. Nakatsuji, and H. Suzuki. Application of probe-vehicle data for real-time traffic-state estimation and short-term travel-time prediction on a freeway. *Transportation Research Record*, 1855:49–59, 2003.

[17] F.P. Terpstra, G.R. Meijer, and A. Visser. Intelligent adaptive traffic forecasting system using data assimilation for use in travel information systems. The Symposium on Professional Practice in AI, First IFIP Conference on Artificial Intelligence Applications and Innovations AIAI-2004, August 2004.

[18] C. Paniconi, M. Marrocu, M. Putti, and M. Verbunt. Newtonian nudging fo a Richards equation-based distributed hydrological model. *Advances in Water Resources*, 26(2):161–178, 2003.

[19] I. Strub and A. Bayen. Weak formulation of the boundary conditions for scalar conservation laws: an application to highway traffic modelling. *Int. J. Robust Nonlinear Control*, 16:733–748, 2006.

[20] Y. Ishikawa, T. Awaji, and K. Akimoto. Succesive correction of the mean sea surface height by the simultaneous assimilation of drifting buoy and altimetric data. *Journal of Physical Oceanography*, 26:2381–2397, November 1996.

[21] R.J. LeVeque. *Finite Volume Methods for Hyperbolic Problems*. Cambridge University Press, Cambridge, U.K., 2002.

[22] S.K. Godunov. A difference method for numerical calculation of discontinuous solutions of the equations of hydrodynamics. *Math. Sbornik*, 47:271–306, 1959.

[23] L. Muñoz, X. Sun, R. Horowitz, and L. Alvarez. A piecewise-linearized cell transmission model and parameter calibration methodology. In *Proceeding of the Transportation Research Board (TRB)* 85th *Annual Meeting*, Washington D.C., January 22-26 2006.

[24] `http://ngsim.camsys.com/`.